

## Bi-directional Lower Hybrid Current Drive and Electron Cyclotron Counter Current Drive Experiments in Full Current Drive Plasma in TRIAM-1M

H. ZUSHI, K. HANADA, H. IDEI, S. NISHI<sup>1)</sup>, T. MAEKAWA<sup>2)</sup>, M. AZUMI<sup>3)</sup>, A. FUKUYAMA<sup>2)</sup>, S. KUBO<sup>4)</sup>, T. SHIMOZUMA<sup>4)</sup>, T. NOTAKE<sup>4)</sup>, K. SASAKI<sup>1)</sup>, B. BHATTACHARYAY<sup>1)</sup>, K. NAKASHIMA<sup>1)</sup>, H. HOSHIKA<sup>1)</sup>, M. SAKAMOTO, M. OGAWA<sup>1)</sup>, K. NAKAMURA, K.N. SATO, M. HASEGAWA, S. KAWASAKI, H. NAKASHIMA, A. HIGASHIJIMA, K. TOI<sup>4)</sup>, Y. TAKASE<sup>5)</sup>, T. SHIKAMA<sup>5)</sup>, S. KADO<sup>5)</sup>, O. MITARAI<sup>6)</sup>, K. TAKAHASHI<sup>3)</sup>, K. TAKAKI<sup>1)</sup>, N. MAEZONO<sup>1)</sup>, M. KITAGUCHI<sup>1)</sup>, F. WANG<sup>1)</sup>, H. Xu<sup>1)</sup>, Y. NOZAKI<sup>1)</sup>, Y. WATAYA<sup>1)</sup>, N. KIMURA<sup>1)</sup>

Advanced Fusion Research Center, Research Institute for Applied Mechanics, Kyushu University, Kasuga 816-8580, Fukuoka, Japan,  
 Interdisciplinary Graduate School of Engineering Sciences, Kyushu University<sup>1)</sup>,  
 Kyoto University<sup>2)</sup>,  
 Japan Atomic Energy Agency<sup>3)</sup>,  
 National Institute for Fusion Science<sup>4)</sup>,  
 The University of Tokyo<sup>5)</sup>,  
 Kyushu Tokai University<sup>6)</sup>  
 E-mail: [zushi@triam.kyushu-u.ac.jp](mailto:zushi@triam.kyushu-u.ac.jp)

**Abstract.** Combined experiments with lower hybrid (LH) and electron cyclotron (EC) waves have been performed to study the counter current drive in LHCD plasma. With injection of backward (BW) LHW counter current drive depends on the power ratio of BW LHW and forward (FW) LHW ( $P_{\text{BWLH}}/P_{\text{FWLH}}$ ). For  $P_{\text{BWLH}}/P_{\text{FWLH}} < 1$ , counter-CD is confirmed by the reduction of the driven current. A transition in current drive scheme occurs near  $P_{\text{BWLH}}/P_{\text{FWLH}} \sim 1$  and the net increase in co current is observed for  $P_{\text{BWLH}}/P_{\text{FWLH}} > 1$ . Relativistic resonant interaction between BW-ECW and counter-passing electrons is confirmed by acceleration in hard X-ray energy spectrum. This interaction, however, cause the current in co-direction to enhance by  $\sim 50\%$ . The dependence of the resonance location is studied. For inboard off-axis condition counter current drive with large Shafranov shift is achieved, but for on-axis and outboard off-axis cases increment in co current is obtained. For on-axis condition, however, net counter-current is achieved as  $P_{\text{BWLH}}/P_{\text{FWLH}}$  increases. Ohkawa scheme is plausible for outboard off-axis case.

Email of H. Zushi: [zushi@triam.kyushu-u.ac.jp](mailto:zushi@triam.kyushu-u.ac.jp)

### 1. INTRODUCTION

Physics understanding for the non-inductive current ramp-up scenario using lower hybrid wave LHW with a spectrum gap between the thermal velocity of electrons and the phase velocity, and establishing a control method of the non-inductive current profile by means of counter current drive (ctr-CD) methods are inevitable for ITER [1]. For relativistic resonant electrons the two kinds of counter current drive experiments by combination of LHW and electron cyclotron wave ECW have been performed in the full current drive plasma sustained by forward (FW) LHW in TRIAM-1M ( $R \sim 0.84\text{m}$  and  $a \sim 0.11\text{m}$ ). FW waves drive the co current in the clockwise direction and backward (BW) one are used to drive the counter current in the counter clockwise direction. Two LH current drive systems are used to launch both LHWs. Fundamental X-mode ECW is injected into such a LHCD plasma through a remote steering corrugated antenna from the low field side in the mid plane.

Three experimental scenarios have been studied. First, the effects of BW-LHW on FW-LHCD plasma are investigated, that is, it is studied how the BW-LHW develop counter streaming

energetic electrons and how the driven current ( $I_{CD}$ ) is modified if BW power ( $P_{LHBW}$ ) is larger than the FW power ( $P_{LHFW}$ ), as shown in Fig.1. So far bi-directional LHCD experiments have been done on Versator II [2] and WT-3 [3], and they have shown that high poloidal beta plasma has been achieved when  $I_{CD}$  was comparable to the Alfvén critical current  $I_A = (17\text{kA}) \gamma v_{\parallel}/c$ , where  $\gamma$ ,  $v_{\parallel}$ , and  $c$  are relativistic factor, electron velocity parallel to the magnetic field and light velocity, respectively. However, no net current reduction has been reported under steady state conditions. On TRIAM-1M a clear net current reduction has been observed, which is considered to be due to the counter current [4]. In the present paper the power ratio of  $P_{LHBW}$  to  $P_{LHFW}$  is extended to  $\sim 1.5$ .

Second, coupling of the fundamental oblique X-mode ECW to the energetic electrons carrying counter-current is investigated as a function of  $P_{BWLH}/P_{FWLH}$ . BW-ECW is injected so as to couple to these electrons. Although the 1<sup>st</sup> X-mode launched from the low field side cannot access the cyclotron layer, wave damping on energetic electrons can be possible by properly choosing the injection angle to satisfy the relativistic cyclotron resonance condition [5, 6], as shown in fig. 2. The thermal electrons in this condition are shielded by the cutoff layer. In TS [7], co-CD by the 1<sup>st</sup> O-mode ECW injection into LHCD plasma is studied under steady state condition and the synergy effect on ECCD is investigated. Although the counter-CD of ECW has been studied in many tokamaks in order to investigate the stability of the neoclassical tearing mode [8, 9, 10], the coupling efficiency to energetic electrons is not studied. In the present paper at the power ratio  $P_{BWEW}$  to  $P_{FWLH}$  of  $> 2$  the counter-CD by BW-ECW is investigated as a function of  $P_{BWLH}/P_{FWLH}$ .

Third, the effect of Ohkawa mechanism [11] is studied for counter-CD by BW-ECW. It is possible for BW-ECW to drive counter-current ( $co-I_{CD}$ ) if they can interact with counter-passing electrons near the passing – trapped boundary. It has been reported in ref. [12] that the outer off-axis resonance condition is favorable for Ohkawa current drive (OKCD). In this paper, in order to distinguish the Fisch-Boozer current (ECCD) [13] and OKCD,  $B_t$  is changed for the relativistic resonance condition to be satisfied inboard side, on-axis and outboard side, while conditions for LHW are fixed. For former two cases since no or few trapped particles exist near the resonance region in the mid plane, Fisch-Boozer counter- $I_{CD}$  can be expected, while for the outboard off-axis condition it is expected that OKCD ( $co-I_{CD}$ ) becomes effective [12].

This paper is organized as follows. In section 2 experimental conditions and both counter current drive scenarios for LHW and ECW are described. In section 3 the results of BW LHW for counter-CD will be presented. In section 4 the coupling of BW-ECW, counter-CD and change in the resonance location will be discussed as a function of  $P_{BWLH}/P_{FWLH}$ . Discussion and summary will be given at section 5.

## 2. Experimental Conditions and Counter Current Drive Scenarios

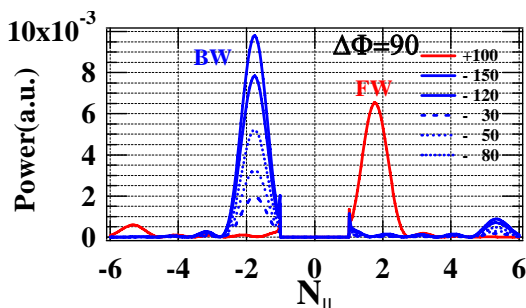


FIG. 1 Power spectra for FW (red) and BW (blue) LHWs. The antenna phasing is  $\pm \pi/2$ .

Two sets of the 8.2 GHz system having 8 klystrons of 25 kW each are used. Both BW and FW LHWs are launched from these identical grill antennas, which are toroidally separated by 180°. The phasing of grided antenna is  $\pm 90^\circ$ , whose peak refractive index  $N_{\parallel}^{\text{peak}}$  is  $\sim \pm 1.65$  corresponding to resonant electron energy of 100 keV. The spectra with the width  $\Delta N_{\parallel}/N_{\parallel} \sim 1$  is shown in Figure 1. The  $P_{FWLH}$  is fixed at  $\sim 40\text{kW}$ . In this experiment the target plasma is sustained

for  $\sim 10$  s by FW-LHW in steady state. BW-LHW is injected at the stationary phase.  $P_{\text{BWLH}}$  is varied in time with the maximum rate of the power ramp up being  $\sim 80$  kW/s and the maximum power ratio is  $\sim 1.5$  during the bi - directional CD phase.

Under these experimental conditions the launched LHW can penetrate into the whole region because of high  $B_t$ , high frequency and low density  $\bar{n}_e < 1 \times 10^{19} \text{ m}^{-3}$ . The critical refractive index  $N_{\text{acc}}$  for accessibility and the up-shifting of LHW refractive index  $N_{\text{up}}$  due to high aspect ratio of  $\sim 7$  and high  $q(>8)$  do not affect the wave propagation. Thus the phase velocity of the up-shifting wave is still about 13 times larger than the electron thermal velocity  $v_{te}$ . That is, there exists a large ‘spectral gap’ between them [14]. Although there exists an extremely large spectrum gap between the thermal electrons with  $T_e = 0.3\text{-}0.4$  keV and energetic resonant electrons with  $\sim 100$  keV,  $I_{\text{CD}}$  of  $\sim 30$  kA can be sustained for  $\sim 180$  s at  $P_{\text{LH}} \sim 50$  kW and hard X-ray measurement perpendicular to the magnetic field lines shows the evidence of energetic electrons extending to  $\sim 200$  keV.

BW- ECW with parallel refractive index ( $N_{\parallel}$ )  $\sim -0.3$  in the fundamental X-mode at 170 GHz

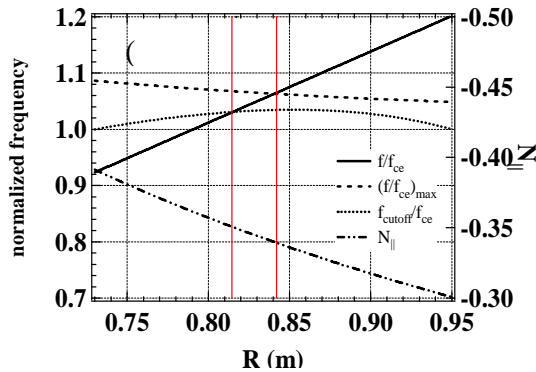


Fig.2 Resonance (dashed), cutoff (dotted) and refractive index  $N_{\parallel}$  (two dotted chained) for  $B_t=6$  T at  $R=0.8$  m and  $n_{e0} = 1 \times 10^{19} \text{ m}^{-3}$ . The parabolic density profile is assumed. Two vertical lines indicate the resonance window.

is launched from the low field side by means of the symmetric remote steering antenna [15, 16]. Two grooved mirror polarizers are located in the transmission line to optimize the elliptical polarization for the oblique X-mode injection. The electron cyclotron resonance  $f=f_{ce}(R_{\text{ecr}})$  is not accessible for the 1<sup>st</sup> X-mode wave launched from the low field side because of the right hand cutoff. Obliquely injected X-mode waves propagate near the cutoff region, bend parallel to the toroidal magnetic field, and reflect towards the plasma edge. The cutoff position  $R_{\text{cutoff}}$  is given by

$$(f / f_{ce})_{\text{cutoff}} = \frac{1}{2} \left( 1 + \sqrt{1 + 4 \frac{f_{pe}^2}{f_{ce}^2} \frac{1}{1 - N_{\parallel}^2}} \right),$$

where  $f_{pe}$  is plasma frequency. However, even for  $R > R_{\text{cutoff}} > R_{\text{ecr}}$  the relativistic resonance condition  $f / f_{ce} = \frac{1}{\gamma(1 - N_{\parallel}v_{\parallel}/c)}$  can be satisfied at  $R_{\text{res}} (> R_{\text{cutoff}})$  for the energetic electrons.

ECW can interact strongly with the resonant electrons because wave electric vector rotates in the same direction as the electron gyration. Since  $f/f_{ce}(R_{\text{res}})$  is larger than unity in the low field side, the resonance condition for negative  $N_{\parallel}$  can be satisfied for electrons carrying ctr current ( $v_{\parallel} < 0$ ).

The largest resonant major radius  $R_{\text{res}}^{\text{max}}$  is given by  $(f / f_{ce})_{\text{max}} = 1 / \sqrt{1 - N_{\parallel}^2}$ . Thus, in the spatial resonance window ( $R_{\text{res}}^{\text{max}} > R > R_{\text{cutoff}}$ ) interaction becomes possible, as shown in Fig.2. In velocity space a pitch angle window also exists to satisfy the relativistic resonance condition. The thermal electrons at  $R_{\text{ecr}}$  cannot be coupled with ECW because of the evanescent layer of a few cm.  $B_{t0}$  is varied from 5.33T to 6.095T, corresponding to inboard off-axis, on-axis and outboard off-axis conditions.  $P_{\text{EC}}$  is fixed at  $\sim 80\text{-}100$  kW, and electron density  $\bar{n}_e$  is kept  $\sim 0.6 \times 10^{19} \text{ m}^{-3}$  so that the ECW can propagate the outer resonance edge.

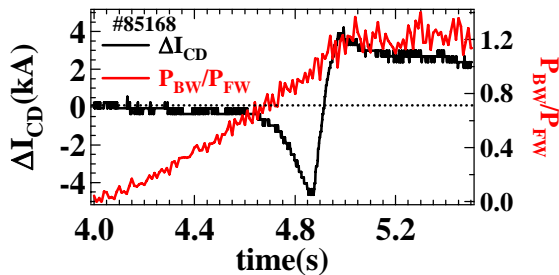


FIG.3 Change in driven current and power ratio  $P_{BW}/P_{FW}$  are plotted as a function of time.

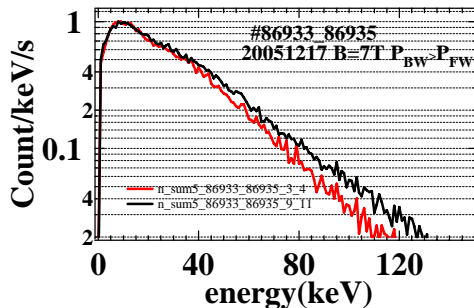


FIG.4. Hard X-ray energy spectra for FWLH (red) and FWLH+BWLH(black) cases. The sampling time is 1 sec.

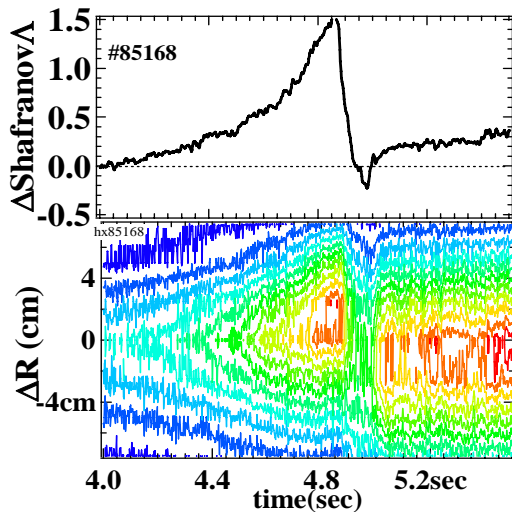


FIG. 5 Change in Shafranov  $\Delta$  and contour plot of the HX intensity profile are shown.

### 3. Bi-directional Current Drive with BW and FW LHWs

First, it is found that co- $I_{CD}$  driven by FW-LHW decays very slowly with increasing  $P_{BWLH}/P_{FWLH} < 0.6$ , it reduces rapidly for  $0.6 < P_{BWLH}/P_{FWLH} < 1.0$ . Finally the reduction in co- $I_{CD}$  is  $\sim 15\%$ . In Fig. 3 the variation in  $I_{CD}$  and  $P_{BWLH}/P_{FWLH}$  are plotted as a function of time. This reduction is considered to be due to ctr-  $I_{CD}$  driven by BW-LHW. Since the pitch angle scattering time of electrons with energy 100 keV is less than 50 ms under present condition, the velocity distribution function ( $f(v_{\parallel}, v_{\perp})$ ) at steady state can be expected to extend both in  $v_{\parallel} < 0$  and high  $v_{\perp}$  out from the resonant region ( $v_{\parallel} \sim c/N_{\parallel}^{peak}$ ) [17, 18]. The perpendicular HX measurement supports the extension in high  $v_{\perp}$  region qualitatively, as shown in fig. 4.

Second, it should be noted that a reduction in co- $I_{CD}$  driven by FW-LHW is accompanied with peaking of  $j(r)$ . The change in Shafranov  $\Delta$  ( $\equiv \beta_p + \beta_p^{tail} + l_i/2 - 1$ ) is plotted as a function of time, as shown in Fig.5 (a). Here  $\beta_p$  is poloidal beta of the bulk plasma and  $l_i$  is the internal inductance. Shafranov  $\Delta$  increases gradually for  $P_{BWLH}/P_{FWLH} < 0.8$  and it enhances rapidly for  $0.8 < P_{BWLH}/P_{FWLH} < 1.0$ . During this current reduction phase  $\beta_p$  is evaluated to increase from 0.27 to 0.34 with an assumption of parabolic profiles of  $n_e$ ,  $T_e$ , and  $T_i$ . However,  $\beta_p^{tail}$  increases from 0.6 to 0.77 with assumption of  $c_{\parallel} = 1$  and  $v_{\parallel} = c/N_{\parallel}^{peak}$ . Therefore,  $\Delta\Delta$  is dominated by the change in current profile  $j(r)$ . In Fig. 5(b) the contour of the hard X-ray (HX) radial profile is plotted as a function of time. The HX(R) becomes peak and keeps the peak position constant during the linearly increasing phase, and then a strong outward shift of the peak position is observed. The maximum outward shift  $\Delta r$  of  $\sim 2$  cm in HX(R) is

consistent with the outwards shift of 1.5-2 cm by magnetic measurements. Thus it is concluded that BW-LHW injection causes the large Shafranov shift of the bi-directional LHCD plasma via enhancement in  $\beta_p^{tail}$  by the reduction of  $I_{CD}$ . Furthermore it is found that BW-LHW injection strongly leads peaking in  $j(r)$ . Since  $P_{BWLH}$  increases gradually, the loop voltage does not change. Observed change in the radial HX profile at 80 keV photon energy [4] suggests that the ctr-

current by BW-LHW is induced near the edge and the total current profile ( $j(r)=j_{co}(r)-j_{ctr}(r)$ ) may be centrally peaked.

For  $P_{BWLH}/P_{FWLH} \sim 1.0$ , however, the ctr-CD by BW-LHW is drastically changed.  $\Delta I_{CD}$  increases from negative to positive abruptly and rapid broadening of  $j(r)$  occurs within  $\sim 0.1$  sec. Since negative  $\Delta I_{CD}$  is considered ctr- $I_{CD}$ , it is noted that positive change in  $\Delta I_{CD}$  should be explained by a mechanism leading to enhancement in co-current drive occurs under the bi-directional LHCD. During further 0.1 s  $\Delta I_{CD}$  starts to decay slowly and  $\Delta\Lambda$  becomes small positive. HX intensity is reduced during this phase. After this transition phase ( $\sim 0.2$  s), even for  $P_{BW}/P_{FW} > 1$ , stationary plasma with positive  $\Delta I_{CD}$  (+ a few kA) and small positive  $\Delta\Lambda$  ( $\sim 0.2$ ) with respect to those in FW-LHW is sustained. This phase is maintained for longer duration (several seconds) compared with the current skin time ( $\sim 0.1-0.2$  s). At this transition the negative loop voltage ( $-0.1 \sim -0.2$  V) transiently appears due to  $\Delta I_{CD}/\Delta t \sim +90$  kA/s. Since this voltage disappears within 0.1 s, it is considered that co-CD in stationary phase is not seriously affected by this voltage. The physics for this transition is not resolved yet. Velocity space instability, equilibrium with bi-directional currents, sensitivity of  $f(v)$  on the co-LHCD efficiency may relate.

The broad HX profile with an inward shifted peak is established and maintained stationary. As shown in Fig. 4, two energy spectra at  $\Delta R = -2.5$  cm are shown for FWLH ( $P_{FWLH} \sim 30$  kW) and FWLH + BWLH ( $P_{BWLH}/P_{FWLH} \sim 1.5$ ), respectively. A clear acceleration of the electrons occurs by BW-LHCD. The difference between these spectra is clear inboard side ( $-5 \text{ cm} \leq \Delta R \leq 0$  cm), but is not clear for  $\Delta R \geq 2.5$  cm. This result is consistent with the stationary HX(R) profile with inner shifted peak shown in Fig.5(b), suggesting that energetic electrons are created for  $-5 \text{ cm} \leq \Delta R \leq 0$  cm for  $P_{BWLH} > P_{FWLH}$ .

#### 4. Counter ECCD in Bi-directional LHCD Plasma

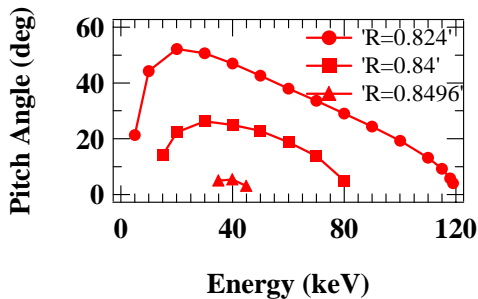


FIG. 6. At three location the resonance condition is plotted in the energy and pitch angle plane.

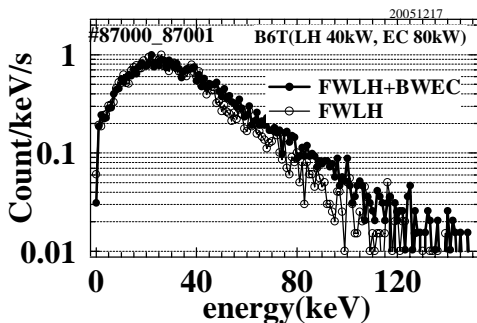


FIG.7. Two energy spectra ; open circles (FWLH) and filled one (FWLH+BWEC).

The relativistic resonance condition is evaluated for BW-ECW with  $N_{||} = -0.3$  under the on-axis condition. As shown in Fig. 6, the wave couples with  $\sim 40$  keV counter passing electrons at the outer edge of the resonance ( $R \sim 85$  cm) and as it approaches to the cutoff layer ( $R \sim 82.4$  cm), the wave can couple with higher energy electrons up to 120 keV. The HX energy spectrum is taken at the on-axis condition. Figure 7 shows that the acceleration is actually occurred by BW-ECW injection in the energy range from 40 keV to 120 keV. Lower energy electrons ( $E \sim 5-10$  keV) can also be resonant with BW-ECW, however, since their pitch angle increases, these electrons are affected by banana trapping.

Figure 8 shows that positive  $\Delta I_{CD}$  (co-current) is observed by BW-ECW for on axis condition. The current increases in the co direction with a time constant of  $\sim 0.1$  s, which is an order of  $L/R$  time, and saturates at  $\sim 16$  kA. This increment in co- $I_{CD}$  is  $\sim 40\%$  of the original



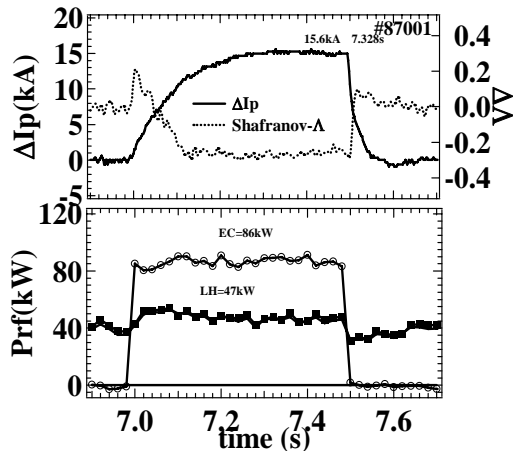


FIG. 8.  $\Delta I_p$ (solid line),  $\Delta \Lambda$ (dotted line) for BW-ECCD on axis. Waveforms of ECW and LHW are also shown.

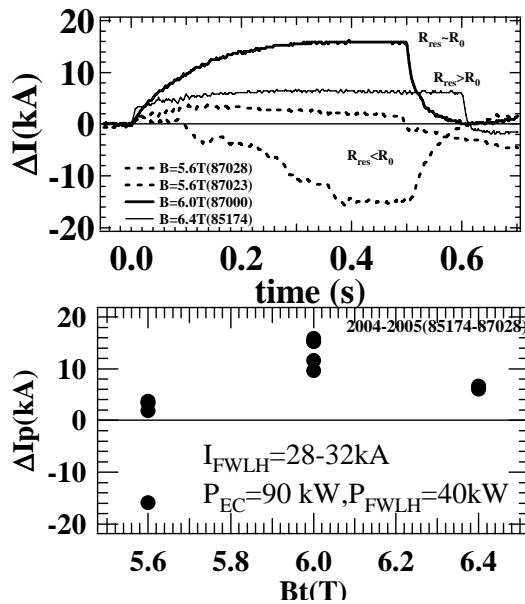


FIG.9.  $\Delta I$  for three resonance positions (inboard off axis, on axis and outboard off axis).  $Bt$  is evaluated at  $R=0.8$  m.

4 ~ -5 cm. On the contrary, for the large negative case, the intensity increases fast and then decreases as  $\Delta I_{CD}$  becomes negative. Furthermore the radial profile shows a remarkable Shafranov shift. Since  $I_{CD}$  becomes less  $I_A$ , this large outward shift of ~ 4cm is ascribed to the enhancement of  $\beta_p^{\text{tail}} > 1$ .

Finally, the effects of the BW-LHW, that is, ctr-passing electrons, on ECCD are studied for the relativistic on -axis resonance case. In the target plasma driven by FW-LHW, BW-LHW are injected at  $P_{BWLH}/P_{FWLH} \sim 0.8$ . As described in the previous section, under this condition a lot of energetic counter passing electrons may exist compared with the case for FW-LHW. The results

LHCD value. Since the power ratio of  $P_{BWEC}/P_{FWLH}$  is  $\sim 2$ , the integrated current drive efficiency  $\eta = nIR/(P_{EC} + P_{LH})$  is reduced to  $\sim 45\%$  compared with the original LHCD efficiency. Shfranov  $\Lambda$  increases fast, then decays with increasing the current, and finally stays constant. This suggests that  $j(r)$  becomes broad as BW-ECW is injected, though the resonance is expected to be on - axis. When the ECW is turned off, the current decays to the original level with a time constant of  $\sim 30$  ms, which is much shorter than the rise time constant. Since the intensity of MoXIII is increased by  $\sim 3.4$  during the EC injection phase, the increment in resistivity may correspond to this fast decay.

The effects of the resonance position on ECCD are studied for inboard off axis, on-axis and outboard off axis cases, as shown in Figure 9. The maximum co- current is achieved for the on axis case. For outboard off axis case,  $\Delta I_{CD}$  is decreased to  $\sim 6$  kA, but still co-current is driven. For inboard off - axis case, there are two typical results, small positive ( $\sim 4$ kA) and large negative ( $-15$  kA). For the former  $\Delta I_{CD}$  increases within 0.1 s, and it turns over and gradually decreases. On the other hand, for the later one, it becomes small positive ( $< 1$ kA) and then decreases gradually and finally stays at the large negative value. The target condition is the same, but for the later case, BW-LHW has been injected for 5 sec and it has been stopped 1 sec before the ECCD is turned on. The HX evolution and radial profile in both cases are quite different. For the small positive case, the intensity increases gradually with keeping the peak position near the resonance position of ~ -

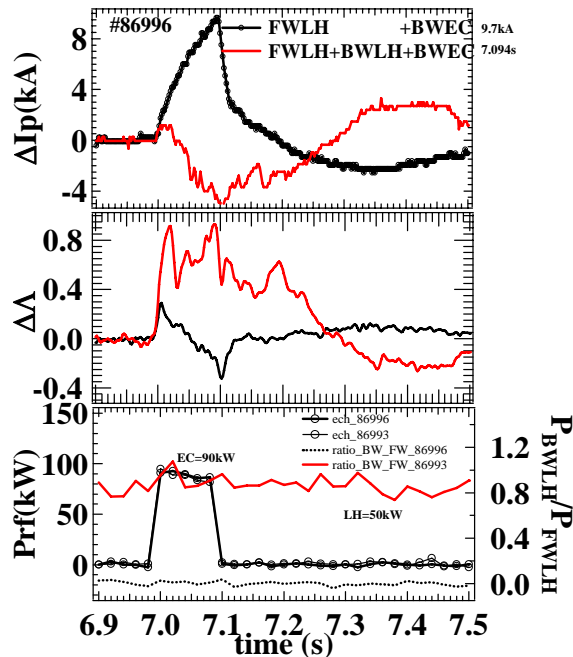


FIG. 10  $\Delta I_p$ ,  $\Delta \Lambda$ ,  $P_{EC}$ , and  $P_{BWLH}/P_{FWLH}$  are shown with (black) and without BWLH (red).

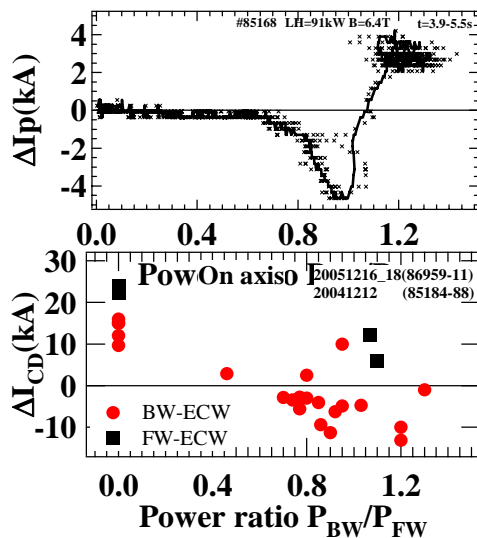


FIG. 11 (a)  $\Delta I$  vs.  $P_{BWLH}/P_{FWLH}$  for bidirectional experiment, (b)  $\Delta I$  vs.  $P_{BWLH}/P_{FWLH}$  for BW-ECW experiment. Squares correspond to ECCD with  $N_{||} \sim +0.3$ .

for on-axis case, because of no trapped particles near the axis. Induced electric field effect also assists the co-current drive. In order to overcome this effect better coupling between BW-ECW and counter-passing energetic electrons is required, and BW-LHW plays an important role to increase the number density of counter passing electrons. Figure 11 shows that BW-LHW tends to enhance the ctr-CD by BW-ECW. Single pass absorption of BW-ECW via energetic ctr-passing electrons driven by FW-LHW is evaluated  $\sim 10\%$  [15] with assumed  $f(v_{||}, v_{\perp})$  in LHCD plasma. With adding BW-LHW single pass absorption will increase [21].

of ctr-ECCD are shown in Fig. 10. For reference the case without BW-LHW is also shown. The change in current is first small positive of  $\sim 1$  kA, and then it starts to decay in the counter direction. The change in  $j(r)$  becomes peaked as suggested by change in Shafranov  $\Lambda$ . In this experiment it was hard to sustain the current constant. One reason is the strong impurity (Mo) product by both injection of BW-LHW and BW-ECW. This is due to the loss of the energetic electrons on the Mo limiter. The hot spot is observed on the limiter and Mo atoms are ejected as the evaporation flux [19].

## 5. DISCUSSION AND SUMMARY

In order to understand the physics of current drive by RF wave the inductive response of the plasma, that is, the transient reversed local electric field has to be considered in addition to the kinetic processes by quasi-linear wave diffusion and Coulomb collision [14]. When the BW-LHW is injected into LHCD plasma, the positive electric field is locally induced. It should be produced via Ohm's law  $E = \eta (J_{tot} - J_{BW})$ , where  $\eta$  is the hot electron resistivity. It has been reported in ref. [20] that close collisions and acceleration lead to 'avalanche-like' runaway production. This assists filling the spectral gap and then enhances the forward current drive efficiency. The transition may be the result of competition of the counter current by BW-LHW and avalanche-like co-current assisted by low electric field. Explanations for long sustainment of the enhanced forward current drive are left for the future.

Although OKCD scheme seems to be a plausible candidate for explanation of co-current for outer off-axis BW-ECCD, the same scheme cannot explain the more positive  $\Delta I_{CD}$

In summary, combined experiments with LHW and ECW have been performed to study the counter current drive in co LHCD plasma. With injection of BW-LHW ctr CD is dependent upon the power ratio of  $P_{\text{BWLH}}/P_{\text{FWLH}}$ . For  $P_{\text{BWLH}}/P_{\text{FWLH}} < 1$ , ctr-CD is confirmed by the reduction of the driven current. A transition in current drive scheme occurs near  $P_{\text{BWLH}}/P_{\text{FWLH}} \sim 1$  and the net increase in co current is observed for  $P_{\text{BWLH}}/P_{\text{FWLH}} > 1$ . Relativistic resonant interaction between BW-ECW and ctr-passing electrons is confirmed by acceleration in HX spectrum. This interaction, however, cause the current in co-direction to enhance by  $\sim 50\%$ . Inboard off-axis, on-axis, and outboard off-axis experiments are done. For inboard off-axis condition ctr-CD with strong Shafranov shift is achieved, but for other conditions net reduction in co current is not obtained. For on-axis condition, however, net ctr-current is achieved as  $P_{\text{BWLH}}/P_{\text{FWLH}}$  increases.

## ACKNOWLEDGMENTS

We would like to thank Prof. T. Maehara for his useful comments on this experiment. This work is partially supported by a Grant-in-Aid for Scientific Research from Ministry of Education, Science and Culture of Japan. This work has been partially performed under the framework of the bi-directional collaboration organized by NIFS.

## REFERENCES

- [1] ITER Physics expert group, Nucl. Fusion **39** (1999) 2495.
- [2] Luckhardt, S.C., et al., Phys. Rev. Lett. **62** (1989) 1508.
- [3] Maekawa, T. et al., Nuclear Fusion **31** (1991) 1394.
- [4] Zushi, H., et al., Nuclear Fusion **41** (2001) 1483.
- [5] Maekawa, T. et al., Phys. Rev. Lett. **70** (1993) 2561.
- [6] Beckmann, M., Leuterer, F., Fusion Eng. Design **53** (2001) 59.
- [7] Giruzzi, G., et al., 2004 *Proc. 20th Int. Conf. on Fusion Energy 2004 (Vilamoura, 2004)* (Vienna: IAEA) CD-ROM file EX/P4-22
- [8] Petty, C.C., et al., Nucl. Fusion (2001) 551.
- [9] Isayama, A., et al., Plasmas Phys. and Cont. Fusion, **42**, (2001) 37.
- [10] Gantenbein, G., et al., Phys. Rev. Lett. **85** (2000) 1242.
- [11] Ohkawa, T., 'Steady-state Operation of Tokamaks by r-f Heating', Rep. GA-A13847, General Atomics, San Diego, CA (1976).
- [12] Decker, J., 'ECCD for Advanced Tokamak Operations Fisch-Boozer versus Ohkawa Methods', in Proceedings of the 15th Topical Conf. on Radio Frequency Power in Plasmas, Wyoming, 2003
- [13] Fisch, N.J. and Boozer, A.H., Phys. Rev. Lett. **45** (1980) 720.
- [14] Fisch, N. J., Rev. of Mod. Phys. **59** (1987) 175-234.
- [15] Idei, H., et al., Nuclear Fusion **46** (2006) 489.
- [16] Zushi, H. et al., Nuclear Fusion **45** (2005) S142.
- [17] Fuchs, V., et al., Phys. Fluids **28** (1985) 3619.
- [18] Bonoli, P.T., Englade, R. C., Phys. Fluids. **29** (1986) 2937.
- [19] Bhattacharyay, R., Zushi, H., Nakajima, K., et al., 17th PSI (2006) P2-78.
- [20] Chiu, S.C., Rosenbluth, M.N., Harvey, R.W., Chan, V. S., Nuclear Fusion **38** (1998) 1711.
- [21] Maehara T., et al., Nuclear Fusion **38** (1998) 39.